CASE STUDY FOR UAS-ASSISTED BRIDGE INSPECTIONS

E.T. Bartczak*, M. Bassier and M. Vergauwen

Department of Civil Engineering,
Faculty of Engineering Technology,
Geomatics Research Group, KU Leuven,
Gebroeders De Smetstraat 1, B-9000 Gent, Belgium
erkkitobias.bartczak@kuleuven.be

Commision II, WG II/8

KEY WORDS: Unmanned aerial systems, bridge, inspection, damage detection, photogrammetry, machine learning.

ABSTRACT:

Bridge inspections are typically expensive and time-consuming, especially in regards of the inspection of difficult-to-reach areas. In recent years, unmanned aerial systems (UASs) have gained attention due to their flexible data acquisition. However, UAS inspections generate large quantities of image and video data, which are currently analysed manually. Additionally, identified damages are currently not assessed accurately in their geometric characteristics and location. In this paper, we propose a time-effective framework for a UAS-based bridge inspection methodology that combines 3D information from photogrammetry and machine learning based object detection to allow direct measurements in the images. Concretely, we propose the use of a two-step flight planning to accurately reconstruct the bridge using limited manual effort. Second, we detect frequently occurring damages such as exposed rebars and concrete spalling on the inspection imagery. Finally, we use the spatial location of the imagery to significantly improve the detection results and geolocate them. We evaluate our proposed framework on a decommissioned concrete bridge. The trained YOLOv8 models prove capable of transfer learning on both our own data and online benchmarks. The photogrammetric reconstruction also proves to be sufficiently reliable. Overall, these are the first steps in automating routine bridge inspections and provide crucial evidence to continue developing the method.

1. INTRODUCTION

The importance of bridge inspections cannot be overstated, as the health of bridge infrastructure directly affects public accessibility, logistics and safety. Despite the crucial role of bridge health, governments struggle to conduct the necessary timely inspections every 3 to 5 years due the typically cost- and time-intensive procedure (Rachmawati and Kim, 2022). To reach essential bridge components such as the under deck, inspectors need to use rappelling or an under-deck bridge inspection truck. These procedures impose significant safety risks for the inspector, are time- and equipment-demanding, and can even lead to costly traffic impairment. Therefore, inspectors are under immense pressure as the inspection process is purely manual. Additionally, inspections lack precise damage quantification, as inspectors are often unable to measure located damages, which can lead to unidentified growth of damages i.e., cracks and corrosion. In some cases, insufficient data acquisition and late maintenance measures lead to bridge closures or even major disasters (Olson et al., 2015; Rania et al., 2019; Baranda Sepúlveda, 2021). Addressing these challenges is crucial for both public safety and economy, as it helps to avoid the immense costs of bridge closures and delayed maintenance measures.

To overcome these challenges, the use of unmanned aerial systems (UASs) for bridge inspections has gained significant attention in recent years. These systems provide a cost-effective and efficient alternative to traditional inspection methods by allowing for the flexible acquisition of high-quality and diverse data in hard-to-reach areas. The use of UASs reduces the risk for inspectors and minimizes the need for bridge closures and traffic disruptions (Kim et al., 2022). Furthermore, advancements such as autonomous object avoidance, highly precise geolocation through real-time kinematics (RTK) GNSS, and multi-sensor equipment have expanded the usage of UASs, while deep learning methods can now be adapted to nearly any task, including the detection of bridge damage. Combining these technologies can significantly reduce routine inspection efforts and free up inspectors for more important follow-up inspections.

Our vision is to develop an automated pipeline for UAS-assisted bridge inspection procedures that improves the data acquisition process especially for hard-to-reach areas and the quality of the extracted damage data. More specifically, we want to use advanced computer vision and machine learning (ML) techniques on the UAS images and the resulting photogrammetric point clouds to conduct an automatic and comprehensive bridge inspection that competes in quality and complexity with conventional routine bridge inspection methods. In this work, we propose a proof of concept on the overall framework for a UAS based bridge inspection, starting with the UAS data acquisition and photogrammetric processing procedure

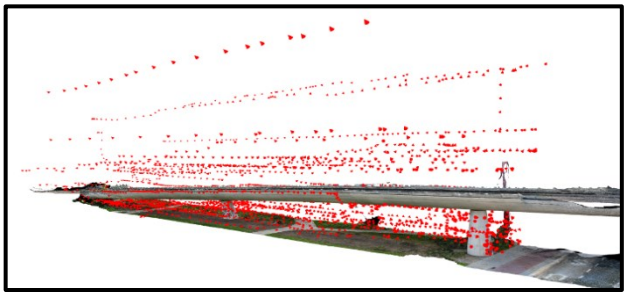

Figure 1: Overview of the polygonal mesh reconstruction of a concrete bridge and the geolocated imagery (red cones) that will be used for the damage localisation and filtering.

* Corresponding author

(§3.1) (**Fig**. **1**). Thereafter, we propose an automated damage detection framework using state-of-the-art ML architectures (§3.2) to both identify potential damage candidates in the images and calculate the 3D coordinates of the prediction bounding box (§3.3). Finally, we suggest image measurement techniques to quantify geometric damage characteristics, i.e., crack width, concrete spalling size or corrosion spot diameter (§3.4). The proposed framework is evaluated in a case study in section 4. The results of the case study are presented in section 5 and the 3D image measurements and future investigations are discussed in section 6.

2. RELATED WORK

In this section, the related work towards automated routine bridge inspections is discussed. Concretely, we present the state-of-the-art in (1) the use of UAS for photogrammetric bridge modelling, and (2) inspection methods based on ML.

2.1 Bridge Inspection

Several challenges still need to be solved to successfully adapt UASs in bridge inspection. The first challenge concerns the time-intensive flight planning and execution for data acquisition. In recent research, this challenge has been addressed by the automatic generation of flight routes based on 3D models, which can be used to facilitate the data acquisition on site (Zhang et al., 2022). However, the generation of optimal flight routes needs to consider the necessary Ground Sampling Distance (GSD) to successfully document minute details, such as concrete cracks. In Liu et al. (2020), the relation between detectable concrete cracks in images and the GSD has been investigated, recommending a 7 times higher resolution than the expected crack width. However, the ideal working distance has still to be researched to address capturing and detecting a diversity of bridge damages. These vary between the types of bridges and inspected components and can include i.e. cracks, spalling, corrosion, missing bolts, or unstable masonry blocks, as well as imperfections such as the growth of vegetation, graffiti, or water stains. Following the data acquisition, the camera positions and 3D models are generated using structure-from-motion (SfM). Toriumi et al. (2021) present an exhaustive review of the state-of-the-art of creating photogrammetric 3D models of bridges using UASs.

A second challenge is the geolocalisation of the close-up inspection grade imagery and 3D reconstruction of bridge models. The current SfM procedures perform excellent in well-lit scenes with sufficient texture detailing i.e., masonry bridges or concrete supports (Zollini et al., 2020). However, near sparsely lighted underdecks, slim railings or reflective steel trusses, current SfM methods underperform (Mandirola et al., 2022). Moreover, inspecting the interior of box girders presents a significant challenge as it poses health risks to inspectors due to the presence of hazardous materials like asbestos and lead coatings. The precise image alignment and 3D reconstruction of the entire bridge is crucial and requires further investigation. This includes the necessary amount of ground control points (GCPs) and their distribution along the bridge, considering the achievable geometric accuracy of the derived bridge models.

2.2 Damage detection

In the past years, various deep learning architectures have been developed to detect damages such as concrete cracks (Hsieh and Tsai, 2020; Munawar et al., 2022; Wan et al., 2022; Wan et al., 2023), steel related damages (Dung et al., 2019; Harweg et al., 2020) and masonry damages (Dais et al., 2021). An extensive overview of available detection models is given in Toriumi et al. (2021). However, these methods are not trained specifically on bridge damage datasets and underperform in these scenarios. Additionally, current methods are very narrowly defined with each method only finding 1-5 types of damages. These frameworks must be drastically expanded to accommodate the wide range of bridge inspection findings, with over 100 different classes ranging from graffiti to concrete cracks. Furthermore, current approaches only consider pixel information for the damage detection. Geometric features must also be considered as they are proven to be vital indicators for material degradations in point cloud analysis (Mohammadi et al., 2019; Xiu et al., 2020; Hake et al., 2022; Momtaz Dargahi et al., 2022). This combination of 2D pixel and 3D point information is highly innovative and still needs to be adapted for bridge inspections. Moreover, the use of other sensors (i.e., infrared (IR), multi-spectral) needs to be explored in this context.

2.3 Damage characterization

After the damage detection step, relevant geometric information characterising the damages needs to be extracted. With the advances in computer vision techniques, multi-class object recognition has found its way to bridge inspections. The application of various computer vision and ML architectures for bridge inspections have been reviewed in Zhang and Yuen (2022). Dong and Catbas (2020) give an overview of general damage characterization algorithms used in civil engineering and conclude a lack of masonry and timber detectors compared to concrete and steel. For concrete cracks, the skeleton method can be used to extract the length and crack width (Liu et al., 2020). This step has not been automated for every damage type. Alternatively, these parameters can be measured manually in the image. However, the measurements are in pixels and need to be translated into metric units. Finally, the extracted damage data needs to be structured and managed. Although building information modelling (BIM) has advanced in the past years, Zhang et al. (2022) conclude a lack of integration within bridge inspections.

3. METHODOLOGY

In this chapter, we propose a framework for UAS based bridge inspections. First, we start with the planning and flight execution procedure of the UAS data acquisition and the photogrammetric reconstruction of the bridge model. Second, we investigate image-based ML architectures on their transfer learning capabilities to identify bridge related damages. Lastly, we propose our strategy to accurately abstract geometric damage characteristics and how they can be used to provide asset managers with valuable information about structural health of the asset.

3.1 Data acquisition and photogrammetric reconstruction

Current path planning algorithms do not account for the appropriate working distances required for different bridge components. For instance, certain areas require close inspection (e.g., pillars), whereas other areas may have lower significance (e.g., deck), or may even need to be avoided entirely (e.g., powerlines). As a result, current generated flight paths lead to both vast amounts of irrelevant data and insufficient image quality for the automated detection of minute damage. For the UAS flight, we therefore propose a two-step approach.

Figure 2: Prediction results with bounding boxes (red) of the YOLOv8 concrete spalling model. The result includes one true positive and two false positive predictions.

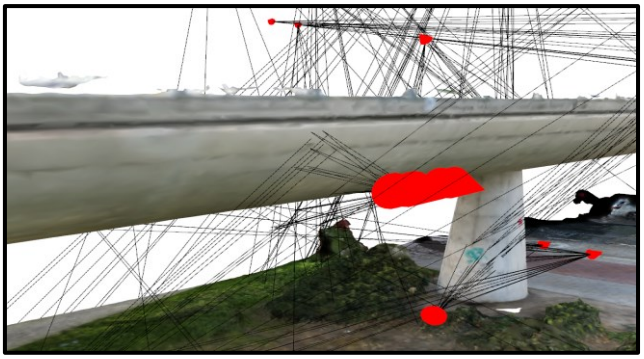

Figure 3: Overview of the damage filtering step: Camera positions (red) and computed projection rays (black).

Concretely, we distinguish between photogrammetric and inspection flights. In the photogrammetric flight, the flight path is optimized for photogrammetric consistency, working with 60 - 90% overlap and an intermediate working distance to the structure to ensure proper alignment and high reconstruction fidelity. Second, we conduct the inspection flight with low overlap at the appropriate working distance for the damages that will be fed to the detection algorithms. The procurement of both flights is kept separate to focus on a single task within each flight. A combination of both flights currently would likely overextend the battery life of the UAS and foregoes a crucial opportunity for the operator to adjust the proposed flight route after an initial mapping is conducted. Additionally, if a prior mapping is already present, only the new inspection flight has to be conducted which significantly lowers the human effort in the field.

For the data processing, we pursue a standalone photogrammetric reconstruction. We aim to reconstruct accurate geolocated photogrammetric 3D bridge models solely based on partial RTK input to drastically lower human effort in the field. First, we process the photogrammetric imagery with a sequential SfM pipeline. We specifically use a low threshold for the matching to align as many images as possible. The reconstruction is scaled and optimized through GCPs. In the test case where we did not yet have the RTK module, we select the lowest number of GCPs to investigate the reconstruction accuracy.

3.2 Machine learning based damage detection

For the detection, we opt for a coarse detection with high recall and filter the results afterwards. For the automated detection, we transfer learn YOLOv8 by Ultralytics (Jocher et al., 2023) (**Fig. 2**). In this first test case, parallel object detection models were trained to predict a number of bridge damage types, i.e., cracks, concrete spalling, exposed rebars, vegetation, graffiti and GCPs. For the training process, we collected images from various sources. Our project partners provided us with a dataset of 140 000 images from bridge inspections including various damage categories. These images came from previous bridge inspections for documentation purposes and therefore contained various quality issues. Many images had red arrows or boxes drawn in the image to help the documentation process of the damages, which makes them impractical for the training process, because it would lead the object detection model to look out for those artificial markings. However, a selection of the images was used for the detection of exposed reinforcement bars and vegetation growth on the bridge. For the graffiti and crack detection models, we used public datasets (University, 2022) and (Zenodo, 2023) respectively. The training images were not domain specific for bridge damages, but contained damages from various constructions. However, it is important to mention that the quality and quantity of training images varied strongly between the categories. During the training process, we iterated between different image, batch and model sizes. The model sizes of YOLOv8 are the nano, medium and large models from ultralytics, which were pretrained on the COCO dataset. The images were annotated manually and a shear rotation of ± 20 ° was applied for data augmentation using Roboflow (2023). We validated the models using the validation function of YOLOv8 and selected the models with the best confusion matrix, i.e. the lowest false negative prediction rate (FN).

3.3 Damage localisation and filtering

Following the detection, the damage candidates are filtered using their spatial relation. To this end, we combine the 3D mesh and the camera positions from the photogrammetric process with the results of the damage detection process to retrieve the 3D location of the detected damages. To this end, we utilized the GEOMAPI python library (Bassier and Vergauwen, 2020) to first compute projection rays. This process uses the information of the camera location, orientation and focal length to compute vectors through the centre point of each bounding box (**Fig. 3**). Second, the intersection points of each ray with the mesh were calculated. If the point can be calculated, it is further investigated which of the segmented components is hit, using the segmented bridge components if present, retrieving sematic information which is added to the damage information. Alternatively, if the damage is not part of the bridge model, it may be considered inconsequential and therefore excluded from further analysis, leading to the erasure of related information. Next, the corner points of the bounding boxes are computed accordingly by backprojecting the damages onto the reconstructed polygonal mesh. The resulting damage information is stored in a RDF graph that can be enriched with the characteristics in the below process (**Fig. 4**).

```
@prefix exif: <http://www.w3.org/2003/12/exif/ns#> .
@prefix v4d: <https://w3id.org/v4d/core#> .
@prefix xsd: <http://www.w3.org/2001/XMLSchema#> .

<file:///9865ae45-c3dc-11ed-9745-c8f75043ce59> a v4d:ImageNode ;
    exif:imageHeight 98 ;
    exif:imageWidth 85 ;
    v4d:confidence "0.655912"^^xsd:float ;
    v4d:damageName "/2 Spalling/Standalone_L_4000_0.3" ;
    v4d:distances "[1.00113    0.99017864 0.998218   1.0062037  1.0148205 ]" ;
    v4d:endpoints """[[ 8.33837793 12.00391319  0.40087332]
 [ 8.32470685 12.02231797  0.41000024]
 [ 8.32229378 11.99287494  0.41094799]
 [ 8.35589584 12.01430932  0.39148758]
 [ 8.3537779  11.98412988  0.3926027 ]]""" ;
    v4d:isDerivedFrom "file:///202_R_Bot_-45_SlantedinFD__147_" ;
    v4d:meshids "[5 5 5 5 5]" ;
    v4d:name "9865ae45-c3dc-11ed-9745-c8f75043ce59" ;
    v4d:roi "(2569, 2654, 1109, 1207)" .
```

Figure 4: RDF Graph representation of the detected damages including the images it was detected in, the confidence and the bridge component.

Figure 5: Cropped out damage with bounding box (left), hand-measurement width (middle) and length of concrete spalling (right).

Figure 6: Gaardeniersbrug, Ghent, Belgium. Typical UAS Image of the initial photogrammetric flight.

Table 1: UAS data acquisition metrics

Flight scenario	WD [m]	Images	Time [h]
1 Photogrammetric flight	20 - 30	356	1.5
2 Inspection flight	0.5 - 5	2880	2.5
3 Additional flight	0.5 - 5	241	0.5

Table 2: Photogrammetric processing metric

Photogrammetric process	Setting	Time [h]
1 Camera Alignment	Low	7
2 Camera optimisation	-	0.25
3 Build dense cloud	Low, mild	12
4 Build mesh	Low	4
5 Texturing	8192 x 16	16

3.4 Damage characterization

After the damage detection, the geometric characterisation of the detected damages is extracted. To this end, the properties of the damage candidates i.e., concrete spalling area or diameter of GCP targets, can be measured using the 3D coordinates. If a pixel-based segmentation is not available, an initial estimation of the geometric characteristics can be conducted manually. First, the bounding box area is cut out from the images and imported in a CAD software. Afterwards, the diagonal of the cropped image is measured in pixel lengths and compared with the actual diagonal length, using the 3D points of the bounding box. After scaling the image on this reference length, the damage characteristics are measured and compared with the hand-measurements (**Fig. 5**).

4. CASE STUDY

To validate the proposed framework, we conduct a bridge inspection using a DJI Mini 3 Pro on a decommissioned concrete box girder bridge (**Fig. 6**). The Gaardeniersbrug was specially chosen because it can be easily reached, has no flight restrictions and several documented visual damages. The inspected bridge section is about 100 m long and included two pillars and the abutment. The focus on this case studies lies within the feasibility of the flight, the accuracy of the photogrammetric bridge model, the damage detection procedure and the evaluation of the accuracy of the image-based measurements.

The two-flight approach was conducted as follows (**Table 1**). First, the photogrammetric images from a working distance (WD) of approx. 20 m for the initial photogrammetric model. After the initial reconstruction, inspection grade images were acquired of the entire bridge from close proximity between 5 to 0.5 m. After the damage detection step, more information deemed necessary and additional flights were conducted. Before the flights, we applied 9 GCPs on the deck, sides and pillars. Additionally, since there were any cracks on this specific bridge, we applied print outs of artificial crack patterns on the bridge, which were designed in a CAD software with known line thicknesses. All images were captured using a commercial DJI Mini 3 Pro with 12 MP camera in manual flight mode and manual focus.

For the photogrammetric process we used Agisoft Metashape (Agisoft, 2023) to register the camera positions and reconstruct the 3D model. The initial model was computed using the images from the photogrammetric flight and updated with the inspection and additional flight images. From the total 3477 images, only 114 images were not be registered successfully, due to insufficient image quality and missing overlap. It is worth mentioning that choosing a lower camera alignment setting resulted in better models, as this allows for higher thresholds in registration uncertainties. **Table 2** shows the used settings for the photogrammetric processing. To scale the model, 9 GCPs were used in a local coordinate system, measured by a terrestrial laser scanner (TLS). Thereafter, we validated the geometric accuracy of the 3D model in a cloud to mesh comparison using CloudCompare (CloudCompare, 2023) (**Fig. 7**). The resulting 3D model was exported and post processed in MeshLab (MeshLab, 2022), including the clean-up from noise and outliers and manual segmentation into the bridge components (**Fig. 8**). After the camera optimisation step in Metashape, the final camera positions were exported as .XML file. **Figure 9** shows the correct registration of images from the inspection flight.

For the ML based damage detection, we trained several YOLOv8 object detection models. In total, 7 models were created of which the training datasets are described in **Table 3**. Since the spalling on the chosen bridge for this study did not show an exposed bar, we collected a dataset not containing an exposed bar from various sources, including Google images and our own. For the artificial crack and the GCP model, we took several images of A4 printouts. To assure the generality of the models, we did not use any images from our data acquisition for the training and validation process. For each detection model, several versions

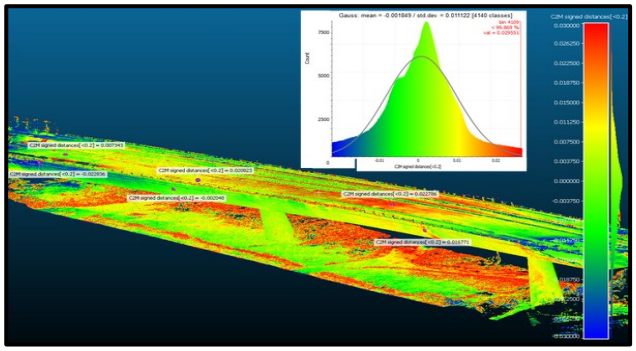

Figure 7: Mesh-to-cloud comparison in CloudCompare using 9 GCPs. The histogram and point measurements indicate a geometric accuracy of about ± 20 mm compared to the TLS.

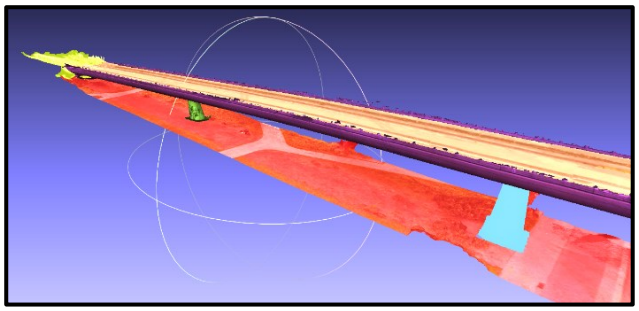

Figure 8: Segmented mesh in bridge components, including the abutment (yellow), middle pillar (green), north pillar (light blue), underdeck (purple), upper deck (orange) and ground environment (red).

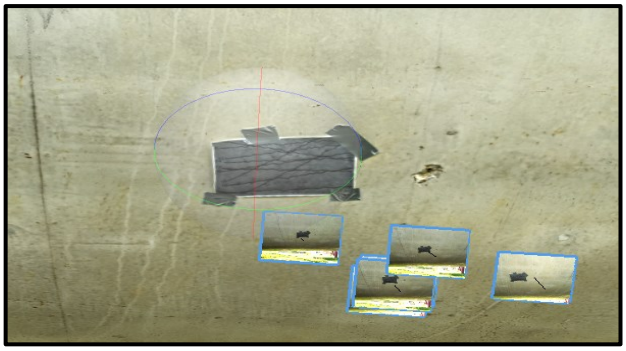

Figure 9: High textureised 3D photogrammetric model, including artificial cracks with line thicknesses ranging between 1.1 to 2.0 mm.

Table 3: Trained YOLOv8 models for different damages

Class	Train Image	R	mAP50	Model size	TP	FN
Cracks	4108	0.783	0.813	Medium	0.84	0.16
Spalling	149	0.998	1	Medium	0.96	0.04
Exposed Bar	161	0.677	0.721	Medium	0.9	0.1
Vegetation	107	0.628	0.661	Nano	0.73	0.27
Graffiti	569	0.61	0.694	Nano	0.7	0.3
GCP	180	0.86	0.866	Large	0.9	0.1
Artificial Crack	141	0.792	0.84	Medium	0.9	0.1

were trained with iterating batch, image and model sizes. However, all the models with the lowest rate of false negative predictions were trained on a batch size of 16 images and an image size of 640 pixels, while the maximal training time did not exceed 300 epochs throughout the process. The largest difference in the model size was observed for concrete spalling, reducing the false negative rate from 0.58 to 0.04.

For the spatial filtering, we back-projected the damages by computing the 3D coordinates of the detected pixels and computing the raycasting intersections with the mesh. For the neighbourhood selection, we used 1 m for the grouping of the damage candidates. For the geometric damage characterization and measurements, we cropped out the bounding box regions from the damage detection process and compared the measurements with the hand measurements. All measurements were conducted manually in the image and the calculated metric values were added to the RFD data management.

5. RESULTS

In this case study, we conducted a UAS based bridge inspection on a case study to validate our proposed framework. From the total 3477 images, only 114 images were not registered in the camera alignment. This shows, that the general flight procedure was successful and can be improved by using automatic flights with more sophisticated flight control settings, ensuring a stable overlap between the images and flight paths.

The photogrammetric 3D model was successfully reconstructed and included a high-quality texture, allowing to visualize detected damages in the 3D context (**Fig. 9**). The cloud comparison with the TLS shows an overall high geometric accuracy. While the histogram shows a mean difference of 1.8 mm, some handpicked points show a difference of approximately ± 20 mm. The largest differences were detected towards the ends of the survey area, which is explained by the lack of images for these regions and furthest distance to the GCPs. The evaluation of the photogrammetric processing showed that highly accurate models can be reconstructed even with less than 9 GCPs per 100 m bridge length. Even if no GCPs were applied in the photogrammetric process, the resulting models could be scaled in a post processing step using only 3 GCPs, while still achieving an overall accuracy of approximately ± 35 mm. However, the photogrammetric model did not include accurate railings and powerlines, which were cleaned up in the postprocessing. Additionally, the bearings on top of the pillars were showed less accurate results and can include errors of up to 8 cm (**Fig. 10**).

The results of the training process of the damage detection models showed a high initial detection rate, even for small training datasets. At the same time, only in the vegetation model a higher false negative prediction rate was observed within the validation data. While the training on larger pretrained model sizes improved the prediction accuracy for the concrete spalling and GCP models, this was not observed for the vegetation and graffiti detection models. From the inspection report, we identified crucial damages and manually selected images of those areas. The trained object detection models were used to predict the damages in this selection of 41 images. The results of the object prediction were saved as .txt file per image, containing the damage type and bounding box information such as centre point values for x and y, width and height of the box in the YOLOv8 format. Each image included multiple detections including false positive predictions. It is worth mentioning that unlike the test images, the validation images were of similar quality as the training data. Therefore, the models produced more false positive predictions on real world data, resulting in 149 damage predictions in 41 images, leading to 98 false positive predictions.

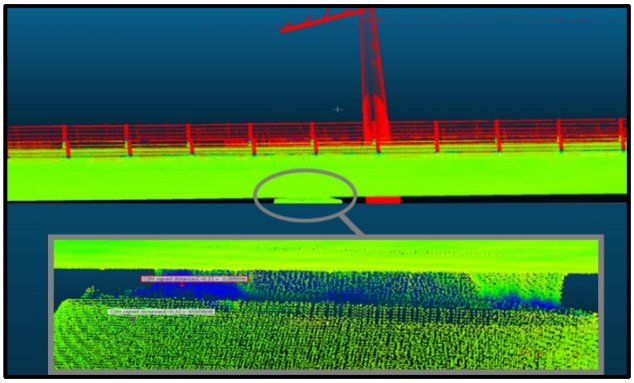

Figure 10: Imperfections of photogrammetric 3D model. Metallic and thin objects such as the railing could not be reconstructed (top, red). The enlarged area (grey, bottom) around the bearings on top of the pillars included less accurate reconstruction (blue).

However, the proposed raycasting method was able to automatically reduce those false predictions in 49 cases. The remaining damage candidates were grouped to damage nodes, containing multiple images from the same damage. This resulted in 36 final damage nodes, which can be accessed and reviewed by bridge inspectors, significantly reducing time effort in the inspection process. Concluding, the models were able to successfully predict all damage instances on the bridge. All damage prediction annotations were automatically combined and stored in the RDF graph for further processing.

Finally, we applied the proposed image measurement method to measure 24 distances in 13 images. **Table 4** shows a selection of these images, the measured damage characteristic, the computed camera distance, the image-based measurement (S_1) and the ground truth measured with a ruler (S_2). The mean measurement accuracy off all measurements ranges between 4.0 to 30.5 mm, if the vegetation damage is considered an outlier and excluded. For these measurements, the camera distance to the damage was about 10 - 12 m, which is one reason for the low measurement accuracy and high absolute a error. Next to the working distance, the accuracy of the image-based measurements depends on several factors i.e., the angle between damage and camera position, the precision of the bounding box, and the geometric accuracy of the bridge model. For larger bounding boxes, especially in complex geometries, this method is not able to deliver accurate measurements. However, for close-up images orthogonal to the damage plane, the results show highly accurate measurements.

6. DISCUSSION

The proposed overall framework was successfully validated in the conducted case study. The results show the great potential of the method to effectively capture high quality images from usually hard to reach areas of bridges, automatically detect bridge damage and extract precise measurements. However, the overall process still allows for further improvements in each of the steps from data acquisition to measurement.

In the data acquisition, the overall image quality will greatly benefit from using more sophisticated UAS compared to the deployed DJI Mini 3 Pro, considering the use of automatic flights to ensure a stable overlap between images and fight paths, while further reducing time effort at the same time. Furthermore, different sensors will be investigated in future research. For the ML process, the results show great potential to train damage detection models. However, it is necessary to improve the overall quality and quantity of training data. To this end, we will investigate the use of weakly supervised learning on large datasets from previous bridge inspections. Lastly, the results of the image-based measurements suggest high potential. The identified influencing factors on the measurement accuracy need to be investigated more profoundly and the extraction will be automated in future research. Overall, the proposed method has great potential to improve current bridge inspection procedures, offering a flexible, time and cost-efficient alternative to the conventional bridge inspection procedure in the future.

Table 4: Direct image measurements and absolute error

Damage ID	Damage character-istic	Camera distance [m]	S_1 [mm]	S_2 [mm]	absolute error [mm]
Spalling_R1	width	1.14	51.0	46.5	4.5
Spalling_R1	length	1.14	98.0	79	19.0
Exposed Bar_1	width	0.64	6.8	8	1.2
Exposed Bar_1	length	0.64	104.4	85	19.4
Vegetation_1	width	12.67	464	470	6.2
Vegetation_1	length	12.67	3036	2200	836.2
GCP_1	diameter_1	6.14	143.5	115	28.5
GCP_1	diameter_2	6.14	169.8	115	54.8
Graffiti_1	length	2.31	160.5	150.0	10.5
Artificial_Crack	width	1.12	2.88	1.90	1.0

7. CONCLUSION

In this paper, we propose a UAS based bridge inspection framework to capture high quality image data, automatically detect and locate potential bridge damage using machine learning and allow for accurate measurements directly in the digital imagery. Furthermore, the pipeline allows to filter out false positive damage predictions, extract semantic data about the bridge components, and group detections of multiple damage candidates into one damage node per damage, allowing for a streamlined data management system. The framework was validated in a case study, successfully detecting an exposed bar, concrete spalling, GCPs, vegetation on the bridge deck and graffiti. The results show great potential of the proposed method, which allowed for millimetre precise measurements of geometric damage characteristics such as crack width, and the automated filtering of the false positive damage predictions.

Author Contributions: E.B. is the main author of the work and conceived the method. M.B. is the direct supervisor. M.V. is the supervisor. All authors have read and agreed to the published version of the manuscript.
Conflicts of Interest: There are no conflicts of interest to report.

8. REFERENCES

Agisoft, 2023. Metashape (Version 2.0.0). Retrieved from https://www.agisoft.com/downloads. (Accessed 24 February 2023).

Baranda Sepúlveda, B., 2021. The Collapsing of Line 12 of the Mexico City Metro. https://revista.drclas.harvard.edu/the collapsing-of-line-12-of-the-mexico-city-metro. (Accessed 17 February 2023).

Bassier, M., Vergauwen, M., 2020. Topology Reconstruction of BIM Wall Objects from Point Cloud Data. *Remote Sensing* 12 (11), 1800. doi.org/10.3390/rs12111800.

CloudCompare, 2023. (Version 2.13). Retrieved from http://www.cloudcompare.org. (Accessed 17 February 2023).

Dais, D., Bal, İ.E., Smyrou, E., Sarhosis, V., 2021. Automatic crack classification and segmentation on masonry surfaces using convolutional neural networks and transfer learning. *Automation in Construction* 125, 103606. 10.1016/j.autcon.2021.103606.

Dong, C.-Z., Catbas, F.N., 2020. A review of computer vision based structural health monitoring at local and global levels. *Structural Health Monitoring* 20 (2), 692–743. doi.org/10.1177/1475921720935585.

Dung, C.V., Sekiya, H., Hirano, S., Okatani, T., Miki, C., 2019. A vision-based method for crack detection in gusset plate welded joints of steel bridges using deep convolutional neural networks. *Automation in Construction* 102, 217–229. doi.org/10.1016/j.autcon.2019.02.013.

Hake, F., Göttert, L., Neumann, I., Alkhatib, H., 2022. Using Machine-Learning for the Damage Detection of Harbour Structures. *Remote Sensing* 14 (11), 2518. 10.3390/rs14112518.

Harweg, T., Peters, A., Bachmann, D., Weichert, F., 2020. CNN-Based Deep Architecture for Health Monitoring of Civil and Industrial Structures Using UAVs. The 6th International Electronic Conference on Sensors and Applications. *MDPI*, Basel Switzerland, p. 69. doi.org/10.3390/ecsa-6-06640.

Hsieh, Y.-A., Tsai, Y.J., 2020. Machine Learning for Crack Detection: Review and Model Performance Comparison. *Journal of Computing in Civil Engineering* 34 (5). doi.org/10.1061/(asce)cp.1943-5487.0000918.

Jocher, G., Chaurasia, A., Qiu, J., 2023. YOLOv8 by Ultralytics. Retrieved from https://github.com/ultralytics. (Accessed 17 February 2023).

Kim, I.-H., Yoon, S., Lee, J.H., Jung, S., Cho, S., Jung, H.-J., 2022. A Comparative Study of Bridge Inspection and Condition Assessment between Manpower and a UAS. *Drones* 6 (11), 355. doi.org/10.3390/drones6110355.

Liu, Y.-F., Nie, X., Fan, J.-S., Liu, X.-G., 2020. Image-based crack assessment of bridge piers using unmanned aerial vehicles and three-dimensional scene reconstruction. *Computer-Aided Civil and Infrastructure Engineering* 35 (5), 511–529. Doi.org/10.1111/mice.12501.

Mandirola, M., Casarotti, C., Peloso, S., Lanese, I., Brunesi, E., Senaldi, I., 2022. Use of UAS for damage inspection and assessment of bridge infrastructures. *International Journal of Disaster Risk Reduction* 72, 102824. doi.org/10.1016/j.ijdrr.2022.102824.

Cignoni, P; Corsini, M; Ranzuglia, G., 2022. MeshLab: an Open-Source 3D Mesh Processing System. *ERCIM News*. Retrieved from https://www.meshlab.net (Accessed 02 February 2023).

Mohammadi, M.E., Wood, R.L., Wittich, C.E., 2019. Non-Temporal Point Cloud Analysis for Surface Damage in Civil Structures. *ISPRS International Journal of Geo-Information* 8 (12), 527. doi.org/10.3390/ijgi8120527.

Momtaz Dargahi, M., Khaloo, A., Lattanzi, D., 2022. Color-space analytics for damage detection in 3D point clouds. *Structure and Infrastructure Engineering* 18 (6), 775–788. doi.org/10.1080/15732479.2021.1875488.

Munawar, H.S., Hammad, A.W.A., Waller, S.T., Islam, M.R., 2022. Modern Crack Detection for Bridge Infrastructure Maintenance Using Machine Learning. *Human-Centric Intelligent Systems*. doi.org/10.1007/s44230-022-00009-9.

Olson, D.W., Wolf, S.F., Hook, J.M., 2015. The Tacoma Narrows Bridge collapse, https://doi.org/10.1063/PT.3.2991.

Rachmawati, T., Kim, S., 2022. Unmanned Aerial Vehicles (UAV) Integration with Digital Technologies toward Construction 4.0: A Systematic Literature Review. *Sustainability* 14 (9), 5708. doi.org/10.3390/su14095708.

Rania, N., Coppola, I., Martorana, F., Migliorini, L., 2019. The Collapse of the Morandi Bridge in Genoa on 14 August 2018: A Collective Traumatic Event and Its Emotional Impact Linked to the Place and Loss of a Symbol. *Sustainability* 11 (23), 6822. doi.org/10.3390/su11236822.

Roboflow: https://roboflow.com. (Accessed 20 March, 2023).

Toriumi, F.Y., Bittencourt, T.N., Futai, M.M., 2021. UAV-based inspection of bridge and tunnel structures: an application review. *Revista IBRACON de Estruturas e Materiais* 16 (1). doi.org/10.1590/S1983-41952023000100003.

University, 2022. Crack Dataset. (Open Source Dataset), https://universe.roboflow.com/university-bswxt/crack-bphdr. (Accessed 12 March 2023).

Wan C, Xiong X, Wen B, Gao S, Fang D, Yang C, Xue S, 2022. Crack detection for concrete bridges with imaged based deep learning. *Science Progress* (10-11); 105 (4) 368504221128487. doi.org/10.1177/00368504221128487.

Wan, H., Gao, L., Yuan, Z., Qu, H., Sun, Q., Cheng, H., Wang, R., 2023. A novel transformer model for surface damage detection and cognition of concrete bridges. *Expert Systems with Applications* 213, 119019. doi.org/10.1016/j.eswa.2022.119019.

Xiu, H., Shinohara, T., Matsuoka, M., Inoguchi, M., Kawabe, K., Horie, K., 2020. Collapsed Building Detection Using 3D Point Clouds and Deep Learning. *Remote Sensing* 12 (24), 4057. doi.org/10.3390/rs12244057.

Zenodo, 2023. STORM graffiti/tagging detection dataset, https://zenodo.org/record/3238357. (Accessed 20 March, 2023).
Zhang, C., Zou, Y., Dimyadi J., 2022. Integrating UAV and BIM for automated visual building inspection: a systematic review and conceptual framework. *IOP Conf. Ser.: Earth Environ. Sci*., 1101 062030. doi.org/10.5281/zenodo.3238357.

Zhang, Y., Yuen, K.-V., 2022. Review of artificial intelligence-based bridge damage detection. *Advances in Mechanical Engineering* 14 (9), 168781322211227. doi.org/10.1177/16878132221122770.

Zollini, S., Alicandro, M., Dominici, D., Quaresima, R., Giallonardo, M., 2020. UAV Photogrammetry for Concrete Bridge Inspection Using Object-Based Image Analysis (OBIA). *Remote Sensing* 12 (19), 3180. doi.org/10.3390/rs12193180.